Figure S1

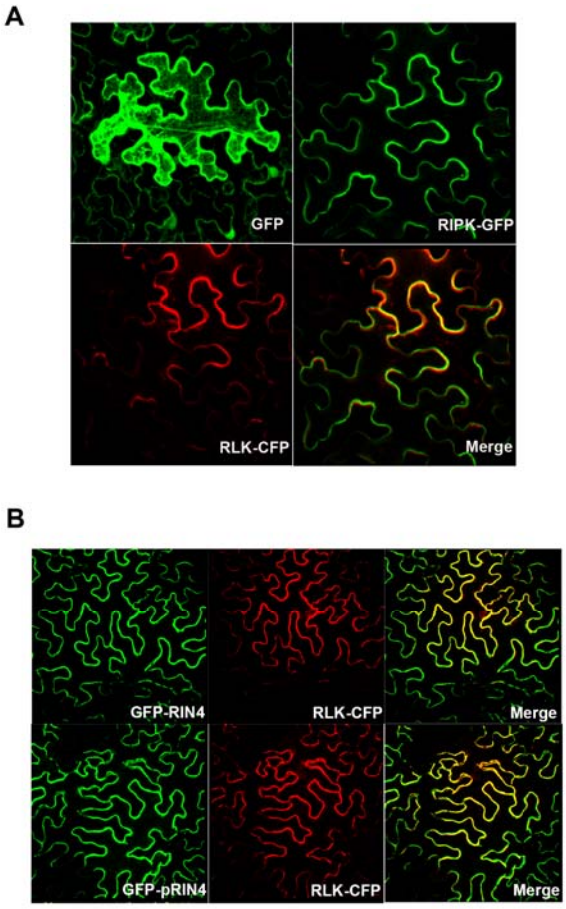

Figure S1, related to Figure 1: RIPK and RIN4 are plasma-membrane localized. Confocal laser scanning microscopy of *N. benthamiana* plant leaves transiently expressing GFP, RIPK-GFP (A), GFP-RIN4, GFP-pRIN4 (B) and the plasma membrane localized protein RLK (At4g23740) fused to CFP on its C-terminus. Depending on the flatness of leaf surfaces, the optical sections of Z-stack were performed at range of 10~16 stacks and thicknesses of the image sections were at range of 11~29 µm. The images shown are representative Z-stacks of GFP and CFP fluorescence. CFP was excited at 415nm and the emission channel was assigned as pseudocolor red. GFP-RIN4, GFP-pRIN4, and RIPK-GFP all co-localize with RLK-CFP in the plasma membrane (yellow, merged color). Images were taken 48h post-infiltration.

Figure S2

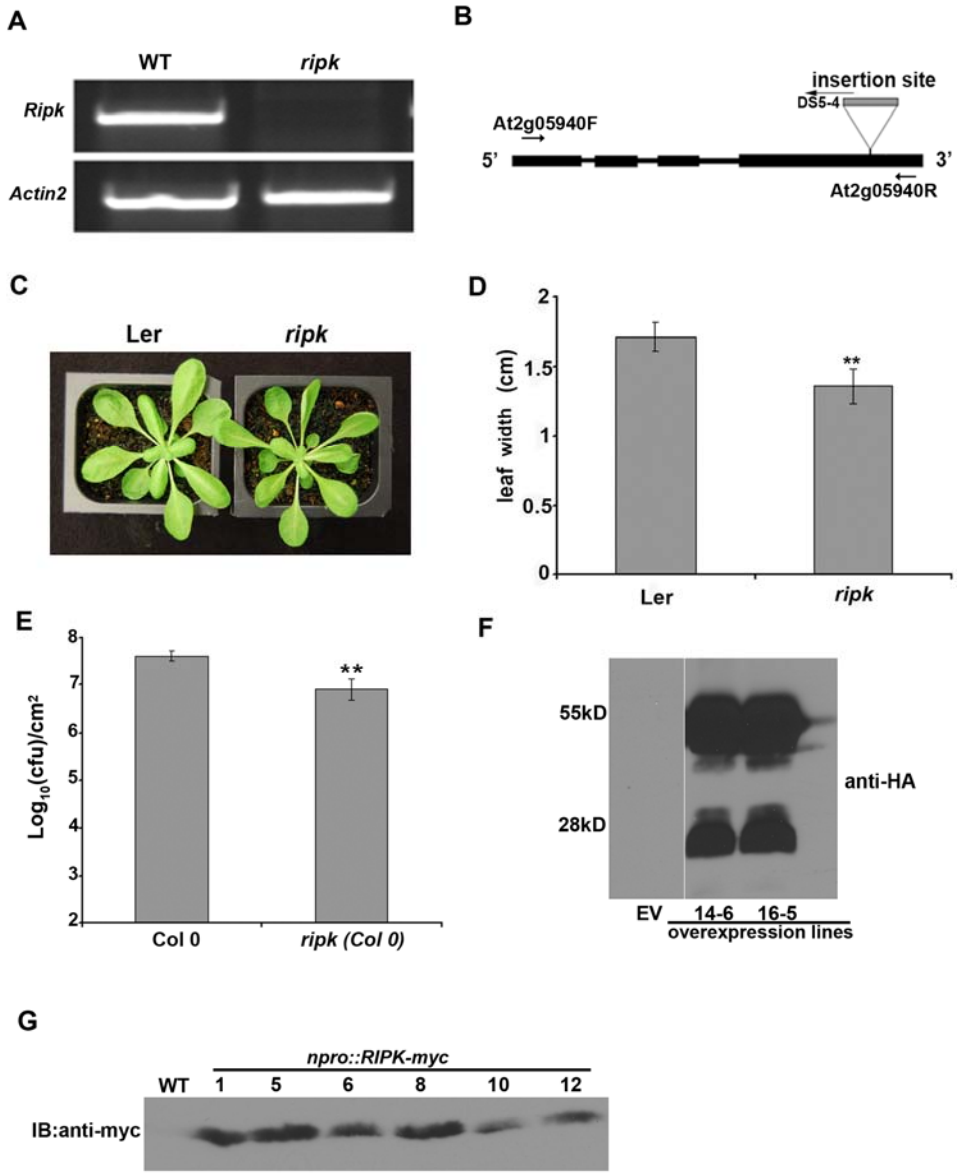

Figure S2, related to Figure 2: The *ripk* knock out line displays narrower leaves and is more resistant to *Pst* DC3000. (A) RT-PCR confirms the RIPK gene is no longer expressed in the T-DNA insertion. Actin2 served as a reference gene. (B) Diagram illustrating the RIPK T-DNA insertion site. Primers used in RT-PCR (At2g05940F/R) and T-DNA screening (At2g05940F/DS5-4) are illustrated. (C) and (D) The ripk knockout exhibits narrower leaves than wild-type L*er*. Error bars represent means ± standard deviation, n = 16. The data shown are representative of two independent experiments with similar results. (E) The *ripk* knockout in a Col 0 background confers enhanced resistance to *Pst* DC3000. Four-week-old plants were spray-inoculated with $1x10^9$ cfu/ml of *Pst* DC3000. Four days post-inoculation, the plants were subjected to growth curve analysis. Error bars represent means ± standard deviation, n = 6. The data shown are representative of three independent experiments with similar results. Statistical differences for (D) and (E) were detected by a two-tailed t-test, alpha = 0.01. (F) Protein expression in *35S::RIPK-HA* overexpression transgenic lines from Figure 2. Anti-HA immunoblots illustrate 35S::RIPK-HA overexpression in Col 0. (G) Protein expression in *npro:: RIPK-myc* complementation transgenic lines. Anti-myc immunoblots illustrate npro::RIPK-myc complementation in *ripk* mutants from Figure 2.

Figure S3

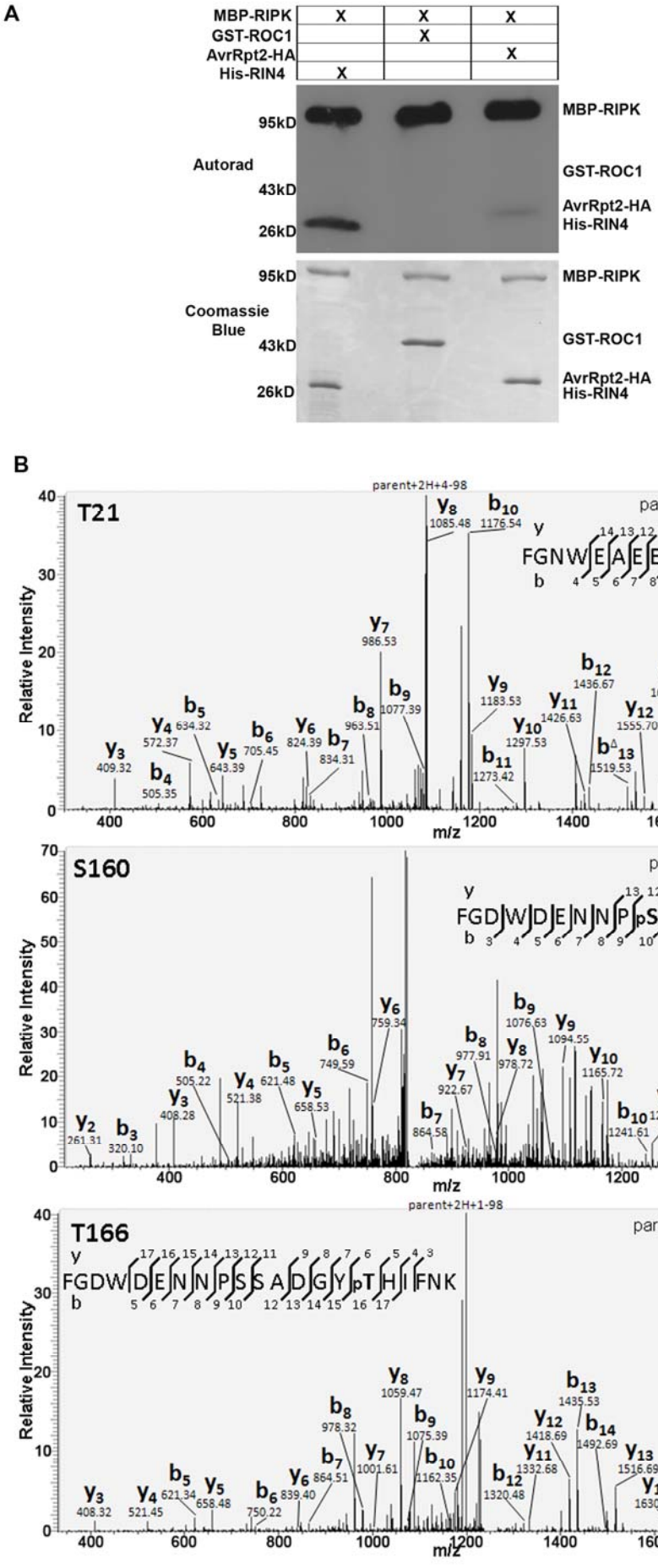
A
MBP-RIPK
GST-ROC1
AvrRpt2-HA
His-RIN4
95kD
Autorad
43kD
26kD
MBP-RIPK
GST-ROC1
AvrRpt2-HA
His-RIN4
95kD
Coomassie Blue
43kD
26kD
MBP-RIPK
GST-ROC1
AvrRpt2-HA
His-RIN4
B
T21
parent+2H+4-98
parent ion m/z = 1130.97 (+2)
FGNWEAEENVPYpTAYFDK
Relative Intensity
m/z
S160
parent ion m/z = 832.01 (+3)
FGDWDENNPpSSADGYTHIFNK
Relative Intensity
m/z
T166
parent+2H+1-98
parent ion m/z = 1248.01 (+2)
FGDWDENNPSSADGYpTHIFNK
Relative Intensity
m/z

Figure S3, related to Figure 3: The substrate specificity of RIPK and identification of RIN4 phosphorylation sites by mass spectrometry. (A) MPB-RIPK cannot efficiently phosphorylate the plant protein cyclophilin ROC1 or the bacterial effector AvrRpt2 *in vitro***.** The kinase assay was initiated by adding γ-32P-ATP to the reaction mixture and phosphorylated proteins were visualized by autoradiography (upper panel). SDS-PAGE gel stained with coomassie blue illustrates protein input (lower panel). (B) Identification of RIN4 phosphorylation sites. Phosphorylation assays (non-radiolabeled) were performed *in vitro* as described in Figure 3 with His-RIN4 and MBP-RIPK in the kinase reaction mixture. Samples were run on a LTQ-FT mass spectrometer and subjected to tandem mass spectrometry. Purified His-RIN4 was run as a negative control to account for any non-specific RIN4 phosphorylation in *E. coli*. Major identified b- and y- ions are labeled on the graphs. Δ represents neutral loss of 98Da (H_3PO_4) on indicated peaks. The upper panel shows fragmentation spectrum (ms2) of precursor ion 1130.97 m/z identifies phosphopeptide FGNWEAEENVPYpTAYFDK (T21). The middle panel shows fragmentation spectrum (ms2) of precursor ion 832.01 m/z identifies phosphopeptide FGDWDENNPpSSADGYTHIFNK (S160). The lower panel shows fragmentation spectrum (ms2) of precursor ion 1248.01 m/z identifies phosphopeptide FGDWDENNPSSADGYpTHIFNK (T166).

Figure S4

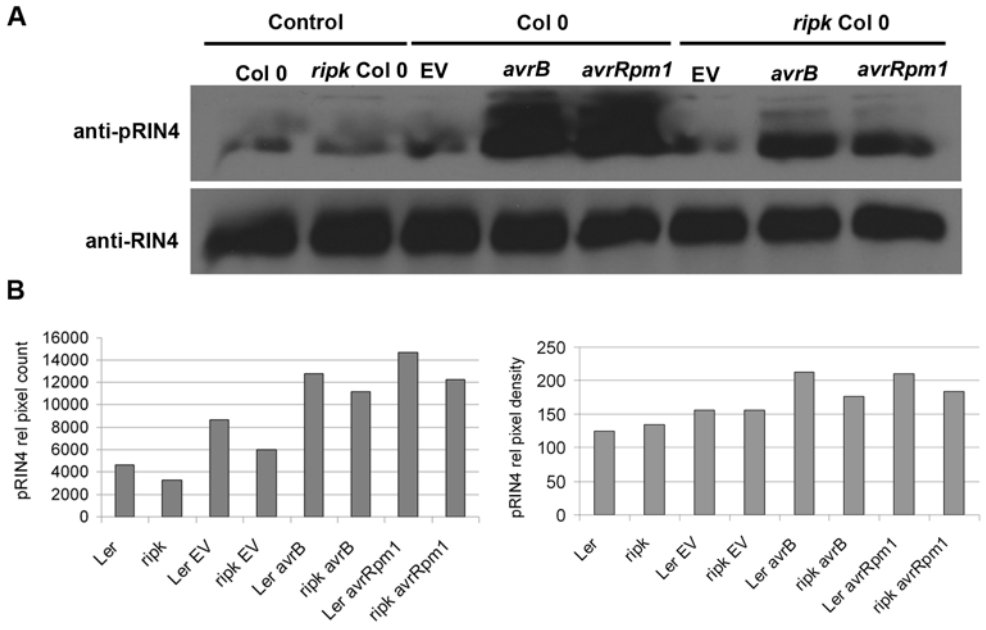

Figure S4, related to Figure 5: Assessing RIN4 phosphorylation in *ripk* Col 0 and quantifying phosphorylation levels in *ripk* L*er*. (A) Arabidopsis leaves were infiltrated with 5x10^{7}cfu/ml of *Pst* DC3000 and *Pst* DC3000(*avrB)* or (*avrRpm1*). Immunoblot analysis was performed 6h post-inoculation. Upper panel = phosphorylated RIN4 immunoblot, lower panel = anti-RIN4 immunoblot, control = 0h time point, EV = *Pst* DC3000 control. Anti-RIN4 blot served as a loading control for anti-pRIN4. (B) Quantification of western blot signals from Figure 5C (*ripk* L*er* verses L*er*). Western blots in Figure 5C were scanned and pixel count (left) as well as band intensity (right) for phosphorylated RIN4 were measured after normalization to the wild-type anti-RIN4 signal.

Figure S5

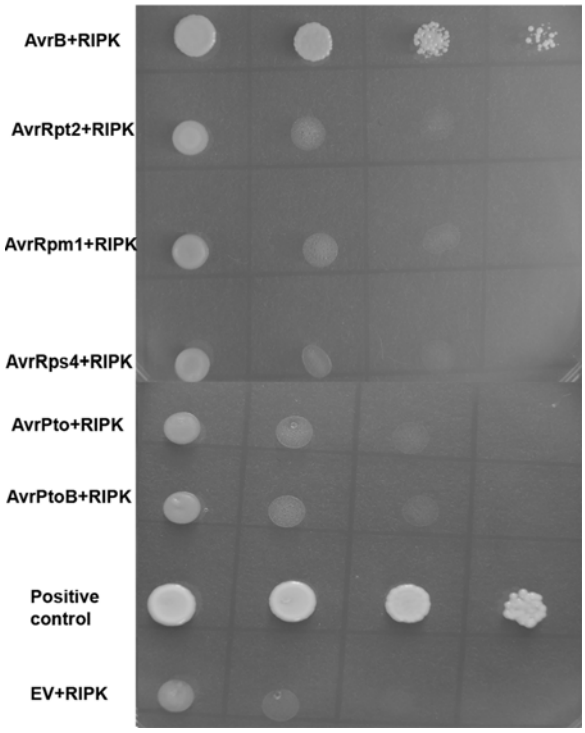

Figure S5, related to Figure 6: RIPK cannot interact with other bacterial effectors by yeast two-hybrid. RIPK was expressed from the BD vector and the effector proteins AvrB, AvrRpt2, AvrRpm1, AvrRps4, AvrPto, and AvrPtoB were expressed from the AD vector (Clontech). pGBKT7-53 and pGADT7-T were used as the positive control. RIPK, RIPK + empty AD vector (EV), and RIPK and respective effectors were co-transformed into yeast and subjected to SD/Leu^-/Trp^-/His^- media selection. The transformed yeast was serially diluted and photographed after 3 days of growth.

SUPPLEMENTAL TABLES

Table S1, related to Figure 1: Proteins identified in the pRIN4 complex by mass spectrometry in Dex::AvrRpm1 (Col 0 background). The number of unique peptides identified in each biological replication is listed.

Identified Proteins (120)	Accession Number	Dex::AvrRpm1 Col 0 (1)	Dex::AvrRpm1 Col 0 (2)	Dex::AvrRpm1 Col 0 (3)	rpm1/rps2/rin4 (1)	rpm1/rps2/rin4 (2)	rpm1/rps2/rin4 (3)
RIN4 RPM1-interacting protein 4	IPI00517440	10	9	12	0	0	0
AT2G05940 Protein kinase (RIPK)	IPI00547996	3	2	0	0	0	0
FTSH1 Cell division protease ftsH homolog 1, chloroplastic	IPI00518805	3	3	5	0	0	0
AT1G20260 V-type proton ATPase subunit B3	IPI00523081	3	3	2	0	0	0
PSBC photosystem II 44 kDa protein	IPI00527600	3	3	3	0	0	0
AAC1 ADP,ATP carrier protein 1, mitochondrial	IPI00546691	3	2	1	0	0	0
AT3G60750 Transketolase-like protein	IPI00537782	11	8	1	0	0	0
LHCB5 Chlorophyll a-b binding protein CP26, chloroplastic	IPI00535216	9	5	6	0	0	0
AT5G01530 Chlorophyll a-b binding protein CP29.1, chloroplastic	IPI00542715	3	1	3	0	0	0
PHS2 Alpha-glucan phosphorylase, H isozyme	IPI00545039	2	12	12	1	0	0
GAPB Glyceraldehyde-3-phosphate dehydrogenase B, chloroplastic	IPI00541680	12	9	5	3	0	0
AT3G14420 Probable peroxisomal (S)-2-hydroxy-acid oxidase 2	IPI00528534	13	10	5	0	0	2
BGLU18 Beta-glucosidase homolog	IPI00521974	6	1	0	0	0	0
ATP1 ATP synthase subunit alpha, mitochondrial	IPI00785805	4	2	0	0	0	0
AT3G08530 Clathrin heavy chain	IPI00544808	3	2	0	0	0	0
AGT Serine--glyoxylate aminotransferase	IPI00540396	3	1	0	0	0	0
SEC6 SEC6	IPI00537390	3	0	1	4	0	3
emb1138 Isoform 2 of DEAD-box ATP-dependent RNA helicase 3	IPI00523172	3	0	2	1	0	0
GS2 Glutamine synthetase, chloroplastic/mitochondrial	IPI00534852	3	0	3	0	0	0
AT5G08690 ATP synthase subunit beta-2, mitochondrial	IPI00516234	2	1	1	0	0	0
GRF2 14-3-3-like protein GF14 omega	IPI00517524	2	1	1	0	0	0
AT2G33800 30S ribosomal protein S5, chloroplastic	IPI00526383	2	1	0	0	0	0
LHCB3 LHCB3 (LIGHT-HARVESTING CHLOROPHYLL B-BINDING PROTEIN 3)	IPI00532626	1	2	2	0	0	0
LOS1 Elongation factor EF-2	IPI00517335	1	2	3	0	0	0
LHCB6 LHCB6 (LIGHT HARVESTING COMPLEX PSII SUBUNIT 6)	IPI00524194	1	2	1	0	0	1
RBCL Ribulose bisphosphate carboxylase large chain	IPI00535114	43	49	41	36	32	28
ATMS1 5-methyltetrahydropteroyltriglutamate--homocysteine methyltransferase	IPI00522440	28	20	20	20	12	14
ATPB ATP synthase subunit beta, chloroplastic	IPI00525776	26	35	37	26	25	22
RCA Isoform Short of Ribulose bisphosphate carboxylase/oxygenase activase, chloroplastic	IPI00518163	21	20	23	10	10	10
CPN60B RuBisCO large subunit-binding protein subunit beta, chloroplastic	IPI00544292	19	23	24	19	20	19
PGK1 PGK1 (PHOSPHOGLYCERATE KINASE 1)	IPI00535490	19	12	15	14	20	15
ATPA ATP synthase subunit alpha, chloroplastic	IPI00540632	18	23	18	16	7	10
CLPC1 CLPC1	IPI00535976	18	19	20	23	8	19
TUB3;TUB2 Tubulin beta-2/beta-3 chain	IPI00525001	18	9	11	7	11	10
CPN60A RuBisCO large subunit-binding protein subunit alpha, chloroplastic	IPI00525237	15	17	14	19	17	15
PEX5 PEX5 (PEROXIN 5)	IPI00545622	14	14	14	9	10	13
GAPA Glyceraldehyde-3-phosphate dehydrogenase A, chloroplastic	IPI00537303	14	12	9	5	3	4
AT5G16810 ATP binding	IPI00543277	13	20	19	15	21	20
TUA4;TUA2 Tubulin alpha-2/alpha-4 chain	IPI00547933	10	7	8	2	1	4
AT1G47550 Exocyst complex component SEC3A	IPI00536614	10	4	9	8	1	10
GAPC2 GAPC2 (GLYCERALDEHYDE-3-PHOSPHATE DEHYDROGENASE C2)	IPI00518090	9	9	11	5	3	4
AT2G02400 Cinnamoyl-CoA reductase family	IPI00542037	8	8	11	5	7	8
VHA-A V-type proton ATPase catalytic subunit A	IPI00525922	8	7	7	3	2	3
PTAC16 PTAC16 (PLASTID TRANSCRIPTIONALLY ACTIVE 16)	IPI00542797	8	4	6	6	2	3
PTAC3 PTAC3 (PLASTID TRANSCRIPTIONALLY ACTIVE3)	IPI00533281	8	4	2	3	4	2
SHM1 Serine hydroxymethyltransferase, mitochondrial	IPI00525727	8	1	0	1	0	0
EIF4A1 Eukaryotic initiation factor 4A-1	IPI00530767	7	6	6	8	5	7
ATPC1 ATP synthase gamma chain 1, chloroplastic	IPI00525302	7	6	7	1	6	2
ATRABE1B Elongation factor Tu, chloroplastic	IPI00520474	7	3	5	5	2	4
- Putative alpha-carboxyltransferase	IPI00527409	6	8	9	8	3	11
MTO2 Threonine synthase 1, chloroplastic	IPI00523359	5	5	6	3	0	4
LHCA3 LHCA3	IPI00532189	5	5	8	2	3	3
HSP60 Chaperonin CPN60, mitochondrial	IPI00533566	5	5	3	2	3	3
CAB2;CAB1;CAB3 Chlorophyll a-b binding protein 165/180, chloroplastic	IPI00527705	4	3	3	2	2	0
RPS1 RPS1 (RIBOSOMAL PROTEIN S1)	IPI00524792	4	1	2	1	3	2
ANNAT4 Annexin D4	IPI00524217	3	4	7	5	4	4
CNX5 Adenylyltransferase and sulfurtransferase MOCS3	IPI00524834	3	3	2	1	1	2
HSP81-2 Heat shock protein 81-2	IPI00537112	3	3	1	1	0	0
EMB2107 EMB2107 (EMBRYO DEFECTIVE 2107)	IPI00519014	2	3	2	5	2	2
AT3G09200 60S acidic ribosomal protein P0-2	IPI00517961	2	3	2	3	2	1
ATPF ATP synthase subunit b, chloroplastic	IPI00536436	2	3	3	0	2	0
GRF1 14-3-3-like protein GF14 chi	IPI00533295	2	2	5	3	3	1
IMPA-2 IMPA-2 (IMPORTIN ALPHA ISOFORM 2); binding / protein transporter	IPI00534241	2	2	2	2	2	1

Identified Proteins (120)	Accession Number	Dex::AvrRpm1 Col 0 (1)	Dex::AvrRpm1 Col 0 (2)	Dex::AvrRpm1 Col 0 (3)	rpm1/rps2/rin4 (1)	rpm1/rps2/rin4 (2)	rpm1/rps2/rin4 (3)
AT5G35430 Binding	IPI00544788	2	1	0	3	0	3
DPE2 DPE2 (DISPROPORTIONATING ENZYME 2)	IPI00538294	2	1	3	2	0	1
TUB8 Tubulin beta-8 chain	IPI00539093	2	1	1	1	1	1
TUB4 Tubulin beta-4 chain	IPI00542050	1	3	3	1	2	2
GRF6 14-3-3-like protein GF14 lambda	IPI00517027	1	2	3	1	3	0
CAT3 AT1G20620 protein	IPI00542721	4	3	3	0	0	2
AT4G34450 Coatomer subunit gamma	IPI00537691	1	1	1	6	1	1
TUB5 Tubulin beta-5 chain	IPI00516743	3	1	2	2	1	1
EIF3C Eukaryotic translation initiation factor 3 subunit C	IPI00522535	1	1	1	2	0	2
GAPA-2 GAPA-2 (GLYCERALDEHYDE 3-PHOSPHATE DEHYDROGENASE A SUBUNIT 2)	IPI00544582	3	2	2	2	0	0
CA1 Isoform 3 of Carbonic anhydrase, chloroplastic	IPI00518464	7	2	4	0	0	0
AT2G26570 Unknown protein	IPI00540846	7	0	0	2	0	0
TIC110 TIC110 (TRANSLOCON AT THE INNER ENVELOPE MEMBRANE OF CHLOROPLAST	IPI00540685	6	9	4	2	0	1
RPN1A RPN1A (26S PROTEASOME REGULATORY SUBUNIT S2 1A)	IPI00529314	6	6	0	3	0	0
ACT7 Actin-7	IPI00524611	5	5	6	3	3	2
ACT8 Actin-8	IPI00524040	10	11	13	10	9	10
LOX2 Lipoxygenase 2, chloroplastic	IPI00548522	10	9	9	3	0	1
AT1G71500 Rieske (2Fe-2S) domain-containing protein	IPI00537413	1	1	4	1	0	0
LHCA4 Chlorophyll a-b binding protein 4, chloroplastic	IPI00523187	1	1	3	0	0	0
PTAC2 Pentatricopeptide repeat-containing protein At1g74850, chloroplastic	IPI00541880	1	0	0	2	1	1
AT4G24830 Argininosuccinate synthase, chloroplastic	IPI00527702	1	0	2	1	1	2
AT5G38430 Ribulose bisphosphate carboxylase small chain 1B, chloroplastic	IPI00521186	1	0	2	0	0	0
HCF136 Photosystem II stability/assembly factor HCF136, chloroplastic	IPI00539527	0	4	3	4	3	4
ADL1 Isoform 1 of Dynamin-related protein 1A	IPI00540791	0	4	1	0	1	7
TUB6 Tubulin beta-6 chain	IPI00545934	0	2	1	2	0	2
PORB Protochlorophyllide reductase B, chloroplastic	IPI00549013	0	2	3	1	0	0
AT4G11380 Beta-adaptin	IPI00516448	0	2	0	1	0	0
AT3G59780 FUNCTIONS IN: molecular_function unknown	IPI00537216	0	2	0	0	1	0
ADL1E Dynamin-related protein 1E	IPI00528678	0	2	0	0	0	3
NSF Vesicle-fusing ATPase	IPI00527613	0	1	1	3	0	0
AT5G25754;AT5G25757 Unknown protein	IPI00532169	0	1	2	2	0	1
SEC8 Probable exocyst complex component 4	IPI00532589	0	1	0	2	0	1
CAD1 Glutathione gamma-glutamylcysteinyltransferase 1	IPI00528107	0	0	0	5	0	0
AT5G02940 LOCATED IN: chloroplast, chloroplast envelope	IPI00533711	0	0	0	5	0	0
AT5G18420 Unknown protein	IPI00525404	0	0	0	4	0	1
NAP1;2 NAP1	IPI00545696	0	0	0	4	0	0
PDX1.1 Pyridoxal biosynthesis protein PDX1.1	IPI00534999	0	0	0	3	0	2
AT4G19006 26S proteasome regulatory subunit	IPI00529601	0	0	0	2	1	1
CIP1 CIP1 (COP1-INTERACTIVE PROTEIN 1)	IPI00524345	0	0	0	2	0	0
AT3G11770 Nucleic acid binding	IPI00530218	0	0	1	1	2	0
TOR1 Microtubule-associated protein TORTIFOLIA1	IPI00530987	0	0	5	1	0	2
RPN12a RPN12a (Regulatory Particle non-ATPase 12a)	IPI00536776	0	0	2	0	4	0
DCP1 mRNA-decapping enzyme-like protein	IPI00517774	0	0	3	0	2	4
TIF3H1 Eukaryotic translation initiation factor 3 subunit H	IPI00526917	0	0	2	0	1	1
ADT2 Arogenate dehydratase/prephenate dehydratase 2, chloroplastic	IPI00528286	0	0	0	0	1	2
AT2G35390 Isoform 1 of Ribose-phosphate pyrophosphokinase 1	IPI00519537	0	0	0	0	1	2
FTSZ2-1 FTSZ2-1	IPI00539833	0	0	2	0	0	1
ESM1 GDSL esterase/lipase ESM1	IPI00547045	3	0	0	0	0	0
VAR2 Cell division protease ftsH homolog 2, chloroplastic	IPI00546467	2	0	0	0	0	0
AOS Allene oxide synthase, chloroplastic	IPI00526231	2	0	1	0	0	0
HSC70-1 Heat shock cognate 70 kDa protein 1	IPI00543293	2	0	0	0	0	0
AT3G14415 Probable peroxisomal (S)-2-hydroxy-acid oxidase 1	IPI00518426	2	0	0	0	0	0
AT1G66840 Protein PLASTID MOVEMENT IMPAIRED 2	IPI00523427	2	0	0	0	0	0
PYK10 Beta-glucosidase	IPI00533497	2	0	0	0	0	0
CRB Uncharacterized protein At1g09340, chloroplastic	IPI00548101	2	0	0	0	0	0
emb1473 50S ribosomal protein L13, chloroplastic	IPI00520181	2	0	0	0	0	0
AT1G30230 Elongation factor 1-delta 1	IPI00531026	2	0	2	3	2	0

Table S2. Primers used in the experiments.

at2g05940F	TTGGATCCATGGCGGTGAAGAAGAAAG
at2g05940R	TTGTCGACTTAGTACCGTTCCCCACCT
RIPKPrF	CACCTAATATTGGAACCGTGAA
A12g05940MYCR	GTACCGTTCCCCACCTGCCTC
2G05940-KINFW	GGGGACAAGTTTGTACAAAAAAGCAGGCTCCATGGCGGTGAAGAAGAA-A
2G05940-KINRV	GGGGACCACTTGTACAAGAAAGCTGGGTCTTAGTACCGTTCCCCACC
At2g05940RHA	TTGTCGACGTACCGTTCCCCACCTGC
AtACT2F	GCCATCCAAGCTCTTCTCTC
AtACT2R	GAACCACCGATACAGACACT
DS3-4	CCGTCCCGC AAGTTAAATATG
DS5-4	TACGATAACGGTCGGTACGG
PrRin4F	CACCTTCTGTCTCTATGAGCATCCATTC
PrRin4R	TAGCTAAAGAATTGAAGTCTGAAGC
RIN4NF	ACGGCGCGCCATGGCACGTTC
RIN4NR	GTGGCGCGCCTCATTTTCCTC
RIPKQF	ATGAGTTCATGCCTCGTGGAA
RIPKQR	AGATAACAGGATTTTCAGCTT
ActinQF	TGG-TGG-AAG-CAC-AGA-AGT-TG
ActinQR	GAT-CCA-TGT-TTG-GCT-CCT-TG

EXTENDED EXPERIMENTAL PROCEDURES

Phosphopeptide mapping by mass spectrometry

Phosphorylated RIN4 (20ug) acquired by a non-radiolabeled *in vitro* kinase assay with RIPK were separated by SDS-PAGE and proteins were reduced, alkylated, and digested with trypsin (Shevchenko et al., 1996). Liquid chromatography tandem mass spectrometry (LC-MS/MS) protein identification was performed using a Waters Nano-Acquity UPLC (Milford, MA) coupled to a hybrid linear ion trap Fourier transform ion cyclotron resonance mass spectrometer (LTQ-FT) (Thermo-Fisher, San Jose CA). Tandem mass spectra data were analyzed using Sequest (ThermoFinnigan, San Jose, CA; version SRF v. 3). Phosphopeptide matches were further validated using Modiro (Protagen AG) (Chamrad et al., 2006) and Ascore (Beausoleil et al., 2006). Phosphopeptide matches were manually validated for peak annotations to exclude incorrect assignments.

Transient Expression in *Nicotiana benthamiana*

Agrobacterium-mediated protein transient expression was performed as described previously (Leister et al., 2005). *T7-RIN4* ORFs*, RIPK-HA*, *avrB-FLAG*, and *GFP* and were cloned into the PMD-1 binary vector (Tai et al., 1999). For HR assays, RPM1 was expressed from its native promoter as previously described (Boyes et al., 1998). The genes of interest in their respective binary vectors were transformed into *A. tumefaciens* strain C58C1. The *Agrobacteria* were infiltrated into *N. benthamiana* leaves at an OD_{600}=0.4. *Agrobacteria* carrying *avrB-FLAG* was infiltrated 24 hours later than all the other genes.

For subcellular localization experiments, *RIN4* and *pRIN4* ORFs were PCR amplified and cloned into the pMDC43 binary vector (Curtis and Grossniklaus, 2003) and fused with an N terminal GFP. *RIPK* was cloned into the pEarleygate 103 vector, with a C-terminal fusion to GFP (Earley et al., 2006). The RLK (At4g23740) fused to CFP has been previously described (Caplan et al., 2009). GFP and CFP fluorescence was observed on a Leica confocal microscope 48 hrs post inoculation. Co-immunoprecipitations were performed as previously described (Krasileva et al., 2010).

Quantification of Western Blot Data

Western blots probed with anti-RIN4 and anti-pRIN4 were scanned and analyzed in Image J (Abramoff et al., 2004). The pixel density and area for phosphorylated RIN4 bands were normalized against wild-type RIN4 to account for differences in RIN4 levels and protein loading.

SUPPLEMENTAL REFERENCES

Abramoff, M.D., Magelhaes, P.J., and Ram, S.J. (2004). Image processing with ImageJ. Biophotonics Internatl. *11*, 36-42.

Beausoleil, S.A., Villen, J., Gerber, S.A., Rush, J., and Gygi, S.P. (2006). A probability-based approach for high-throughput protein phosphorylation analysis and site localization. Nat. Biotechnol. *24*, 1285-1292.

Boyes, D.C., Nam, J., and Dangl, J.L. (1998). The Arabidopsis thaliana RPM1 disease resistance gene product is a peripheral plasma membrane protein that is degraded coincident with the hypersensitive response. Proc. Natl. Acad. Sci. USA *95*, 15849-15854.

Caplan, J.L., Zhu, X., Mamillapalli, P., Marathe, R., Anandalakshmi, R., and Dinesh-Kumar, S.P. (2009). Induced ER chaperones regulate a receptor-like kinase to mediate antiviral innate immune response in plants. Cell Host Microbe *6*, 457-469.

Chamrad, D.C., Korting, G., Schafer, H., Stephan, C., Thiele, H., Apweiler, R., Meyer, H.E., Marcus, K., and Bluggel, M. (2006). Gaining knowledge from previously unexplained spectra-application of the PTM-Explorer software to detect PTM in HUPO BPP MS/MS data. Proteomics *6*, 5048-5058.

Curtis, M.D., and Grossniklaus, U. (2003). A gateway cloning vector set for high-throughput functional analysis of genes *in planta*. Plant Physiol. *133*, 462-469.

Earley, K.W., Haag, J.R., Pontes, O., Opper, K., Juehne, T., Song, K., and Pikaard, C.S. (2006). Gateway-compatible vectors for plant functional genomics and proteomics. Plant J *45*, 616-629.

Krasileva, K.V., Dahlbeck, D., and Staskawicz, B.J. (2010). Activation of an Arabidopsis resistance protein is specified by the *in planta* association of its leucine-rich repeat domain with the cognate oomycete effector. Plant Cell *22*, 2444-2458.

Leister, R.T., Dahlbeck, D., Day, B., Li, Y., Chesnokova, O., and Staskawicz, B.J. (2005). Molecular genetic evidence for the role of SGT1 in the intramolecular complementation of Bs2 protein activity in *Nicotiana benthamiana*. Plant Cell *17*, 1268-1278.

Shevchenko, A., Wilm, M., Vorm, O., Jensen, O.N., Podtelejnikov, A.V., Neubauer, G., Shevchenko, A., Mortensen, P., and Mann, M. (1996). A strategy for identifying gel-separated proteins in sequence databases by MS alone. Biochemical Society Transactions *24*, 893-896.

Tai, T.H., Dahlbeck, D., Clark, E.T., Gajiwala, P., Pasion, R., Whalen, M.C., Stall, R.E., and Staskawicz, B.J. (1999). Expression of the Bs2 pepper gene confers resistance to bacterial spot disease in tomato. Proc. Natl. Acad. Sci. USA *96*, 14153-14158.